A Comparison of Temperature and Humidity Effects on Phosphor Converted LED Package and the Prediction of Remaining Useful Life with State Estimation

Pradeep Lall [(1)], Hao Zhang [(1)], Lynn Davis [(2)]
[(1)]Auburn University
NSF-CAVE3 Electronics Research Center
Department of Mechanical Engineering
Auburn, AL 36849

[(2)]RTI International
Research Triangle Park, NC 27709

ABSTRACT

This paper focuses on the failure mechanisms and color stability of a commercially available high power LED under harsh environmental conditions. 3 groups of the same pc-HB warm white LED were used in the experiment. The first group was subjected to both high temperature, and high relative humidity (85°C/85%RH) with a 350mA bias current. The second group was subjected to only temperature stress at 105°C with a 350mA bias current. The last group was subjected to extreme high temperature 175°C and high bias current (500mA). Samples were taken out from the chamber for both photometric and colorimetric analysis at periodic intervals to investigate the change of the optical parameters. The physics of failure due to the material degradation has been correlated with the change in the photometric and colorimetric parameters of the LED packages. At the end of the experiment, 6000hours of data is projected forward with state estimation methods to compare with projections made with the ~~TM~~ TM-21 method.

Experimental results shows that only optical parts degrades at high temperature conditions. However, at both high temperature and high relative humidity condition, the phosphor layer of the pc-LED can swell and the color stability of LEDs degrades significantly. Also, comparison between TM-21 method and state estimation method shows that state estimation can achieve the same goal with a relatively easy method.

KEY WORDS: Humidity Effects, Accelerated Lift Test, Warm White LED, State Estimation, Remaining Useful Life

NOMENCLATURE

T	Aging Temperature (Kelvin)
Ea	Activation Energy (eV)
X	State Vector
Y	Output Vector
U	Input Vector
V	Process Noise Vector
N	Measurement Noise Vector
f	Transfer function
h	Output function

Greek symbols

Φ	Absolute Radiant Flux (μW/nm)
λ	Wavelength (nm)
α	Decay Ratio

Subscripts

i	Test Condition
k	Time Step

INTRODUCTION

Phosphor converted LEDs are the most preferred method to generate white LED. In this design, blue chips are coated with phosphors to produce a white light spectrum. There are three general classes of white based on the correlated color temperature (CCT) of their light spectrum. CCT of 2700-3500 K (kelvin) are defined as the warm white. CCT of 3500-4000k are described as neutral white and CCT values above 4000K are loosely termed as cool white (blueish white). Phosphor-based LED products can emit different white spectrum due to their unique material properties of various phosphor materials. LED packages with different phosphor coatings can exhibit white spectrum with large variability. Even with the same phosphor materials, various color temperatures can be achieved by adjusting the density of the phosphor particles or the thickness of the phosphor and binder layer.

The main phosphor material used in pc-LED is Y3Al5O12:Ce3+ (YAG:Ce), due to its high quantum efficiency (QE) under the blue LED excitation (90% even under 120°C). Also, the synthesis of YAG:Ce is relative straightforward. The deficiency of pc-LED that use only YAG:Ce is that they are limited to high CCTs and moderate CRIs, due to a lack of red spectral components. This problem can be solved by blending the red Eu2+ nitride phosphor with YAG:Ce phosphor. Phosphor blends of YAG:Ce and GaAlSiN3:Eu2+ combined with blue LED emitter can generate high CRI, warm white LED [1-3].

Most research shows that LEDs rarely fail catastrophically [4-7]. Instead, there are general two failure phenomena. Either their light output degrades slowly over time or the chromaticity coordinates of the LED shift during the operation. Previous research shows that there are at least two predominate degradation mechanisms. One mechanism is the degradation of the LED chip due to the increase of non-radiative recombination which reduces the total number of emitted photons [8-14].The other predominate mechanism is the degradation of the accumulated optical parts from temperature or electric stresses[15-16]. Both of these failure mechanisms could cause the reduction of luminous flux output. Also, degraded optics work as a light spectrum filter and will rescale the intensity of light at each wavelength, which will caused the color coordinates to shift. Besides, increase of non-radiative

recombination of electrons and holes will ~~cause the~~create more heat ~~from~~ in the die region that will worsen the degradation of optical parts of the LED package.

The reliability of high brightness LEDs (HBLEDs) used for illumination have been studied for the past ten years and major findings are reviewed elsewhere. There has also been previous work on other SSL luminaire components such as drivers, but in general there is a lack of publicly available data on humidity effects on LED packages. IESNA (illuminating Engineering Society of North American) published an aging test standard LM80 [17]. LM-80 refers to a method for measuring the lumen depreciation of solid-state lighting sources, such as LED packages, modules and arrays. This standard methodology would allow customers to evaluate and compare the lumen maintenance of LED components from different companies. During the test, LED packages are placed in a temperature controlled case (55°C, 85°C and third temperature) and driven with external current sources. At each readout time, LED are taken out of the thermal chamber to cool to room temperature for both colorimetric and photometric measurement. However, in the ~~LM-~~LM-80 test, only temperature are involved and relative humidity effect are not considered. In LED based luminaire applications, some are operated in the harsh environment. During the operation, the LED package not only experiences the high bias current and ambient temperature, but also the humidity around the package, especially for the road lighting and automobile lighting. Proper design of LED products for different environment requires the understanding of the various effects on LED package from thermal stress and humidity.

In this paper, experiments are set up to explore the different effects of the humidity and the thermal stress on LED packages. Moderate CRI (Ra=80), commercial available warm white (~~3000k~~3000K) LEDs are used to study the degradations caused by temperature and humidity. Each group focuses on either the thermal stress or the combination of thermal stress and humidity. Extreme conditions were intentionally picked ~~up~~ to accelerate the life test. If the test results are the same, it can be proven that humidity had no effects on the LED package and that all the damage in the package ~~would come~~came from thermal stress. On the other hand, if the test results between each groups are not the same, thermal stress and humidity effects can be concluded from each groups. 3 groups of the same pc-HP warm white LED were used in the experiment. The first group (Group1) was subjected to both high temperature~~,~~ and high relative humidity (85°C/85%RH) with a 350mA bias current. The second group (Group2) was subjected to only temperature stress at 105°C with a 350mA bias current. The last group (Group3) was subjected to extreme high temperature 175°C and high bias current (500mA). Test result from the experiment shows that there is huge difference between each groups. Therefore, humidity has a totally different effect on the package compared with the thermal stress. Besides, the thermal stress also has various effects on the LED package with different thermal stress level.

Result from the measured photometric and colorimetric data shows that high relative humidity and high temperature would damage the phosphor and the binder layers on top of the die. Optical images of the phosphor and binder layer indicate that phosphor layer on top of the die expands during the aging at 85°C/85%RH. The ambient temperature and current bias would cause the increase of the junction temperature and degrade the optical parts of the package. Degraded optical parts work as a light spectrum filter and start to absorb more light. If the junction temperature goes up to a certain level, the LED die starts to degrade and the ohmic contact resistant starts to increase. As a result, the characteristic VI curve of the die starts to shift and more and more heat will be generated in the die region. Finally, the whole package will be damaged.

EXPERIMENTAL SETUP

1. Test Vehicle

One kind of commercial available pc-HB warm white LED package was used for the designed test. These LEDs were purchased from LED SUPPLY. Each of the LED packages was pre-soldered on a star board. They were powered up through the solder pads that connect the electrodes inside the package. The star boards can be directly fixed on the aluminum heat sink with screws. The following Figure 1 shows the LED used in this experiment.

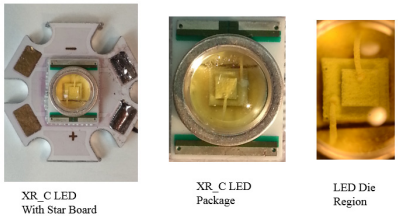

Figure 1: XRC pc HB Warm White LED

LED packages were biased in series with constant current power source. Additional information about the LEDs that were used in the experiments is provided in Table 1:

Table 1: Characteristics of LED Package

Characteristics	Typical Value	Maximum Value
Thermal Resistance	12°C/W	NA
CRI	80	NA
Reverse Voltage	NA	5V
Forward Voltage(350mA)	3.5V	4.0V
Junction Temperature	NA	150°C
Forward Current	NA	500mA
CCT	3000K	3700K

2. Test Setup

During the experiment, a temperature and humidity environmental chamber was used to accelerate the life test of the LED packages. Test procedures followed the protocols that outlined in JESD22-A101C from the electronics industry. This test standard requires constant temperature and humidity. At the same time, test samples were electrically power biased on and off at an interval of one hour in the environmental chamber.

Three groups of samples were prepared for the designed tests and each group had a population of five. Detailed test condition for each group are provided in the Table 2.

Table 2: Test Condition of Each Group

Group	Current	Test Condition	Aging Time
Group1	350mA	85°C/ 85%RH	5708 hours
Group2	350mA	105°C	6360hours
Group3	500mA	175°C	816 hours

Each group was powered in series with constant current power source at designated current. Samples were attached to aluminum heat sink and secured with screws as shown in Figure 2.

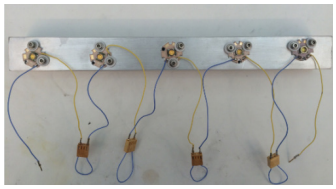

Figure 2: LED Connected in Series on Heat Sink

Three constant test environments were used to check the different effects from temperature and humidity. During the test, each group that mounted on a heat sink were placed in their own environmental chamber for the accelerated life test. The LED package were powered up with a constant current driver that was out of the chamber. After two weeks, 336 hours, the LED packages were moved out of the chamber and cooled down to room temperature. Their photometric and colorimetric properties were measured inside an EVERFINE integrated sphere, following the instructions from LM-79 test standard [18]. Before the measurement, the instruments (integrating sphere and spectroradiometer) were calibrated against a reference standard calibrated for total spectral radiant flux. Photometric values and electric characteristics of LED packages are all sensitive to temperature and air movement. It is important to have a thermal equilibrium environment for the measurement. Samples that attached to a small fin heat sink were operated for 10 minutes to achieve thermal stability, before the absolute radiant flux spectrum were taken. All measurements were taken in a 4 π geometry with the sample located in the middle of the sphere. Measurement setup including connectors, spectroradiometer are shown in Figure 3.

Figure 3: Measurement Setup

Characteristic curves of the diodes were measured with KEITHLEY 2401 power source. Sweep current changed from 0mA to 500mA and forward voltage was measured. VI curves of the LEDs were plotted with the measured data to monitor the electrical properties of the dies. After electrical properties were measured, all samples were returned to the environmental chamber for further accelerated life test. The measurements includes correlated color temperature, absolute radiant flux and color render index (CRI). Also, some other parameters were calculated based on the measured data, such as color shift distance, luminous flux and radiant power. All measured and calculated parameters are listed in Table 3.

Table 3: Measured and Calculated Parameters

Measured	Calculated
• Absolute Spectral Radiant Flux (μW/nm) • Correlated Color Temperature(K) • Color Coordinates in Chromaticity Diagram(u' v') • VI Curve	• Luminous Flux (lumen) • Radiant Power (W) • Color Shift Distance • Photon number (1/s) • Yellowness Index • Yellow to blue ratio

EXPERIMENTAL RESULT AND DISCUSSION

3 groups of the same pc-HB warm white LEDs were used in the experiment. Each group had a population of 5. Absolute radiant flux is measured with spectroradiometer and integrating sphere in μW/nm. Absolute radiant flux of each visible wavelength was plot together as a spectrum. Test result of one sample from each group were plotted below and other samples have the same trend. Figure 4, Figure 5 and Figure 6 show the measured absolute radiant flux spectrum of Group1, Group2 and Group3.

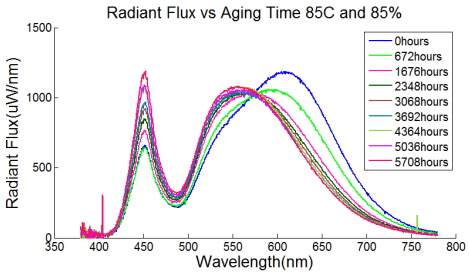

Figure 4: Absolute Radiant Flux Measurement of Group 1

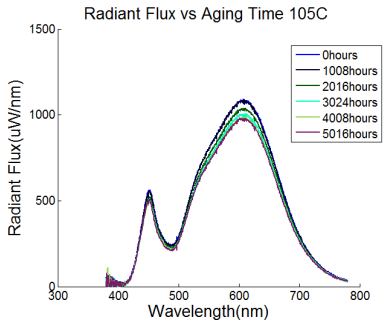

Figure 5: Absolute Radiant Flux Measurement of Gorup2

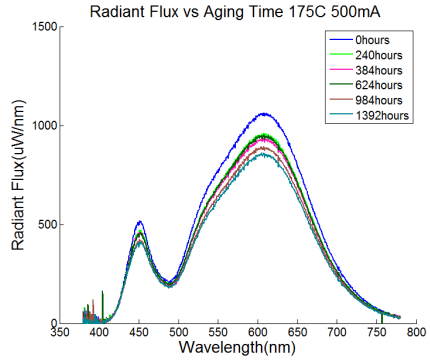

Figure 6: Radiant Flux Measurement of Group3

Changes of the absolute radiant flux spectrum have different patterns compared with each group. The difference indicates that there are various failure mechanisms that are caused by the relative humidity and the temperature stress. Figure 4 demonstrates that the absolute radiant flux of phosphor emission from Group1 shifts to the lower wavelengths during the aging under 85C/85%. The shift of the spectrum indicates the significant change in the phosphor material. During the high and extreme high temperature aging, there is no sign of a similar spectral shift. This comparison can conclude that the humidity will alter the phosphor material and cause the shift of radiant flux spectrum.

From the measurement of Group2 and Group3, a degradation of the absolute radiant flux over the aging time can be observed. Also, from the observation, there is no sign of a shift in the yellow peak spectrum which means that the phosphor is still functioning well after high temperature aging. Figure 6 demonstrates a dramatic drop in the blue peak compared with Figure 5 which indicates a degradation of the blue emitter during the extreme high temperature aging. It can also be concluded that higher temperature will lead to a higher decay ratio of the absolute radiant flux spectrum by comparing the Figure 5 and Figure 6.

The luminous flux maintenance of each group as a function of aging time is shown in Figure 7. Each color represents the average value of a unique group that contains five samples. The test duration is approximately 6000 hours, except for the Group3. All samples of Group3 failed after a short time (less than 2000 hours), due to the extreme high junction temperature. Test result of Group1 demonstrates that the luminous flux actually increases during the 85C/85% aging. This finding is in agreement with the absolute radiant flux spectrum measurement. The absolute radiant flux spectrum of Group1 shifted to the left during the accelerated life test and it will be scaled more by the photopic sensitivity equation. As a result, the calculated luminous flux will increase.

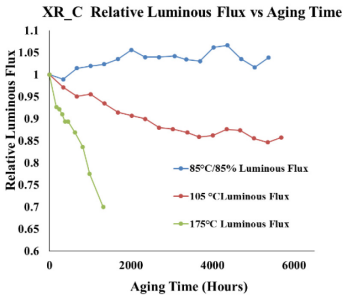

Figure 7: Relative Luminous Flux vs aging time

In contrast, a decline in luminous flux was observed for the Group2 and Group3. The result is in agreement with the measurement of the absolute radiant flux also. Another way to examine this is to check the radiant power of LED package. Radiant power is calculated by the integration of absolute spectral radiant flux without the scale of photopic sensitivity equation. The radiant power of all three groups should decrease, due to the degradation of optical parts and the blue light emitter. Figure 8 demonstrates the change of radiant power over the aging time. The test result shows that high temperature will lead to high decay ratio of the radiant power. The blue emitter of the package will degrade according to the ambient temperature. Less photons will be emitted by the degraded emitter at higher junction temperature.

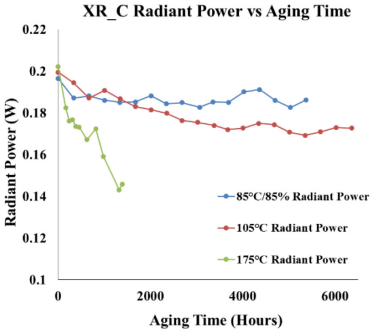

Figure 8: Radiant Power Change with Aging time

In CIE (International Commission on illumination) 1976 u' v' chromaticity space, each LED color was represented by a pair of u', and v' coordinates. The American National Standard

(ANSI) defines the specifications for the chromaticity of solid state lighting products. The existing chromaticity standard (ANSI C78.376) for compact fluorescent lamps (CFL) is based on six nominal correlated color temperatures. For SSL products, quadrangles are used for the chromaticity criteria [19]. If the color coordinates shift out of the designated quadrangle, the color change is visible for human. Marking the test result of the chromaticity coordinates in 1976 CIE chromaticity space shows the color shift path during the accelerated test [20-21]. Chromaticity coordinates of each readout time is connected by arrows.

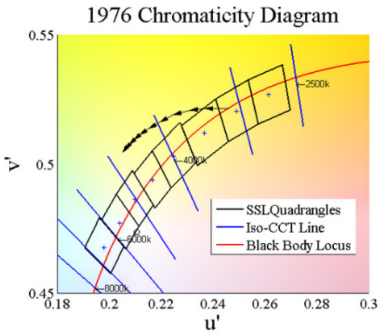

Figure 9: Color Shift Path of Group 1

Figure 9 shows the color shift path of Group1. At the beginning of the accelerated test, the CCT value of the LEDs sits inside the 3000k SSL quadrangle. After exposing to high humidity for a very short time, the CCT value shifts out of the 3000K SSL quadrangle towards the green direction. Such a green shift can be defined by a decrease in u' and minimal change in v' Additional humidity exposure causes a shift that heads increasingly toward the blue direction (defined as a decrease in both u' and v'). This finding provides clear evidence for a change in the phosphor layer. The quadrangles are the criteria for each nominal CCT value. If the CCT value of LED package shifts out of its initial quadrangle, the LED package will be defined as failed in color stability.

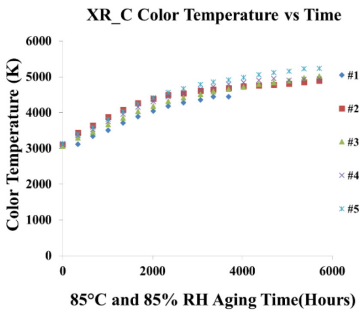

Figure 10: Correlated Color Temperature of Group 1

Humidity will lead to an increase of the CCT value of LED packages. As show in Figure 10, the CCT value of the LED package under 85°C/85% aging condition increased dramatically. However, the CCT value of the LED packages under high temperature do not change as much over the time as shown in Figure 11.

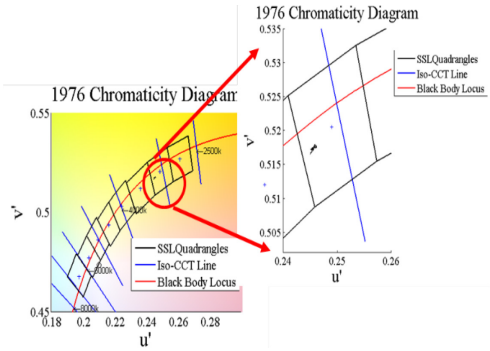

Figure 11: Color Shift Path of Group 2

Color Shift Distance is the absolute distance between the accelerated tested LED package's chromaticity coordinates and the pristine LED package's chromaticity coordinate in the CIE 1976 color space. Monitoring the color shift distance helps to monitor the color stability of the LED package and build the health management system. Color shift distance calculation is given by equation (1). Figure 12 shows the test result of color shift distance.

$$\Delta u'v' = \sqrt{(u_i - u_o)^2 - (v_i - v_0)^2} \qquad (1)$$

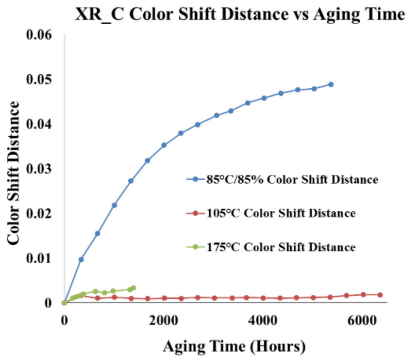

Figure 12: Color Shift Distance vs Aging Time

An LED is a semiconductor device which consists of a p-n junction. When it is forward biased, it will pass current. The forward current and forward voltage are in an exponential relation. Measuring the characteristics curve of the LED package helps to monitor the p-n junction inside the package. During the accelerated life test, at each readout time, the VI

curve of the samples had been taken. The test result can be used to check if there is any material or electric change of the diode. The following Figure 13 shows the test result of one sample from Group1. Test results of other samples in Group1 have the same pattern.

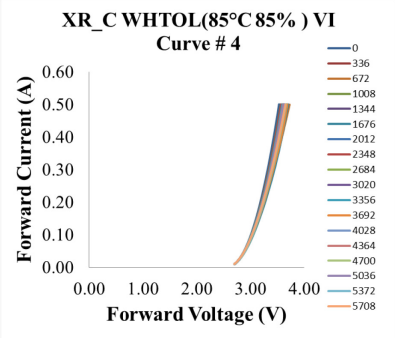

Figure 13: Group1 VI Curve Test Result vs Aging Time

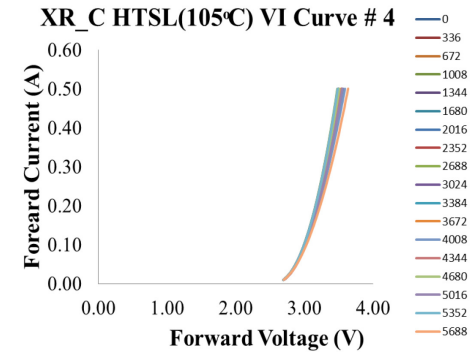

Figure 14: Group 2 VI Curve Test Result Vs Aging Time

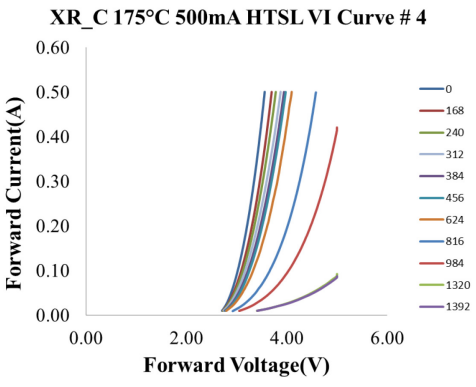

Figure 15: Group 3 VI Curve Test Result vs Aging Time

Figure 13 and Figure 14 demonstrate that there are no monochromatic pattern of the change in the VI curve during the accelerated life test. It can be concluded that electric properties of the diode were very stable during the test. The conclusion is in agreement with the absolute radiant flux measurement of Group1 and Group2. However, in Figure 15, an obvious VI curve shift can be observed. This is also consistent with the absolute radiant flux measurement of Group3. Dramatic changes of the VI curve means that the electric or material change of the diodes has occurred inside package. That also explains the big drop of the blue peak radiant flux of the samples in Group3.

FAILURE MECHANISMS ANALYSIS

Figure 16 provides the optical image comparison between the controlled sample and the sample which has been aged for 5780 hours under 85°C/85% test condition. The die region of the two samples has also been examined in the right part of Figure 16. All the optical images were taken under the same light conditions. As shown below, the color of the die region changed from reddish yellow to light yellow. The color change of the phosphor is evidence of the dramatic shift of the chromaticity coordinates shown in Figure 9.

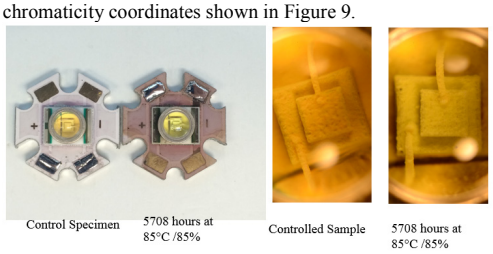

Figure 16: Comparison between the Controlled Sample and the Failure Sample

In order to further study the failure mechanisms of warm white LED package under accelerated life test, a controlled sample and a failed sample from each group were cross sectioned in the middle of the package. On the cross section surface, the die, phosphor and binder layer, encapsulation and the dome lens can be observed clearly under the optical microscope and scanning electronic microscope (SEM). Figure 17 in the next page depicts the cross section surface of the controlled sample, sample from Group1 and sample from Group2 in the order from the left to the right. An obvious color change of the phosphor layer was observed for the sample that was exposed to 85°C/85%. Detailed analysis of the phosphor and binder layer in each package was performed under the SEM. Higher magnification images of the phosphor and binder area were taken to examine the failure mechanism. Figure 18 below provides the images from SEM of 273 magnification.

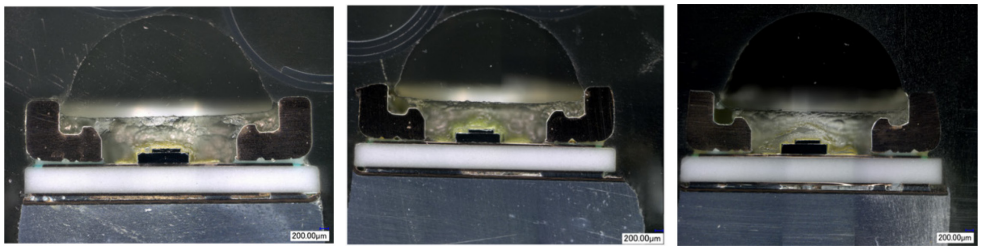

Figure 17: Optical Picture of the Cross Section Surface. The left image is for the controlled sample. The middle one is the optical image of the samples under 85°C/85% for 5708 hours. The right image is for the samples under 105°C for 6360 hours

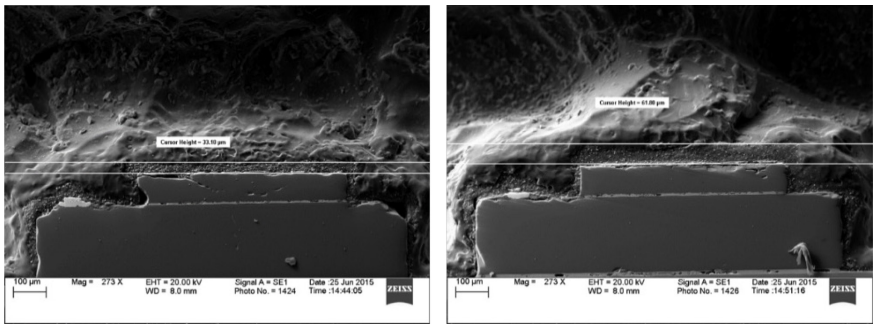

Figure 18: SEM Images of 273 magnification. The left image is for the controlled sample. The right one is the image of the sample under 85°C/85% for 5708 hours

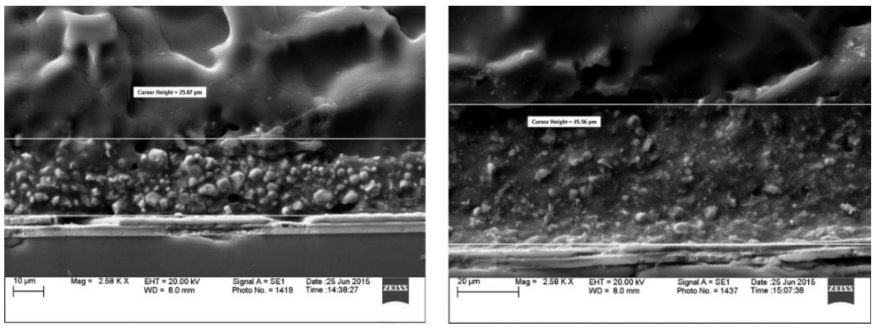

Figure 19: SEM Images of 2580 magnification. The left image is for the controlled sample. The right one is the image of the sample under 85°C/85% for 5708 hours

Commented [DL1]: Note that the scale bar in the picture on the right hand side of Figure 19 is different than the one on the left hand side. This is probably not a big deal here, but you will want pictures with exactly the same scale bar in the future.

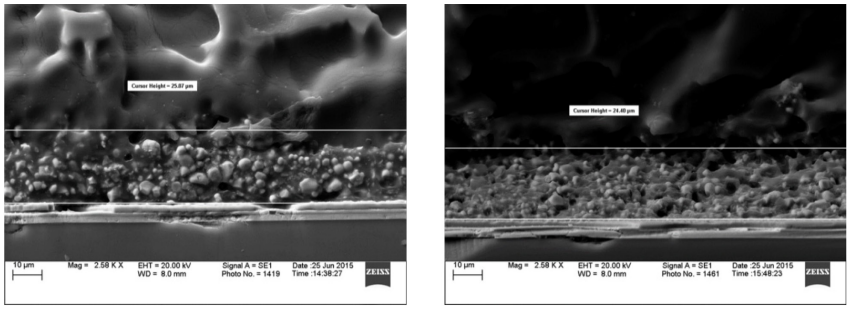

Figure 20: SEM Images of 2580 magnification. The left image is for the pristine sample. The right one is the image of the sample under 105°C for 6360 hours

The thickness measurement of the phosphor layer marked by the white line in Figure 18 indicates the expansion of the phosphor and binder layers during the accelerated life test. The thickness of the phosphor and binder layer changed from 33.10 µm to 61.80µm. In order to observe the phosphor particles, SEM image of 2580 magnification were taken. Figure 19 provides the SEM image of the phosphor particles in the binder layer. All the images were taken under the same working distance and magnification.

In Figure 19 shown above, a variety of the changes of the phosphor particles can been observed. The most obvious one is the density change of the phosphor particles. Phosphor particles are evenly distributed on the top of the thin film blue light emitting die which locates on the top of the sub mount. After exposed to 85°C/85% for 5708 hours, the density of the phosphor particles starts to reduce. This observation is in agreement with the expansion of phosphor and binder layer.

In order to further compare the different effects between the relative humidity and thermal stress. A comparison of the cross section surface between the controlled sample and the sample from Group2 was done under the SEM. Figure 20 provides the SEM image with a magnification of 2580. It can be observed from the above image that the high temperature test environment aging did not change the density of the phosphor particles. Additionally, there is no sign of expansion in the phosphor binder layer. The aged sample have similar thickness of the phosphor binder layer compared with the controlled sample.

REMAING USEFUL LIFE PREDICTION

Usually ~~LM~~ LM-80 report requires 6000 hours' test data. Then, TM-21 long term lumen maintenance projecting method can be used to extend the test data to the desired time [22]. TM-21 method requires at least two test conditions which makes the test very lengthy and tedious. Figure 21 provides the least square curve fit of the data from Group 2 and ~~Gourp3~~Group3. The black line shows the prediction of the luminous flux at 140°C with the measured data.

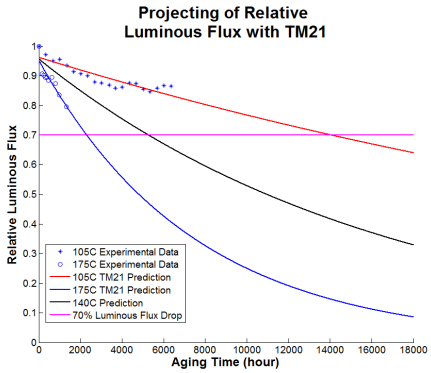

Figure 21: Projection of Relative Luminous Flux with TM21 Method

In order to calibrate the activation energy, TM21 method can only work with two finished tests that been performed under different aging temperature. These estimation and information ~~then,~~ can then be used to assess the expected useful life of other using condition. As shown above, this method is tedious and requires long test data (6,000 hour minimum with >10,000 hours preferred). The data driven approach that has been used in the ~~(~~prognostics health management~~)~~ (PHM) framework, can also be used to estimate the remaining useful life (RUL), especially for the case where the physics based governing equation have not been obtained yet. Compared with the TM21 protocol, the data driven method needs much less data and is much easier to perform. The mathematical model used in the state estimation usually has two master equations. The first is the state transfer equation and the second is the output equation which describes the relationship between the state variables and the output variables. Equation (2) and Equation (3) shows the general state transfer equation and output equation.

$$X_k = f(X_{k-1}, U_{k-1}, V_{k-1}) \quad (2)$$

Where, Xk is state variable vector; k is the current time step and k-1 is the previous time step. Uk-1 is the known input to the system from previous time step; Vk-1 is the process noise of the mathematical model applied to the practical model.

$$Y_k = h(X_k, U_k, N_k) \quad (3)$$

Where, Yk is the output of the system which can be measured with sensors; Nk is the measurement noise during the measurement.

There are two steps during the estimation process. The first step is to perform the filter to the measured data and the second step projects the state vector forward with the transfer function [23]. The state estimator estimates the true states under noise and error. After sufficient training, the estimator can understand the system and works independently without the measured data. The following Figure 22 shows the estimation process.

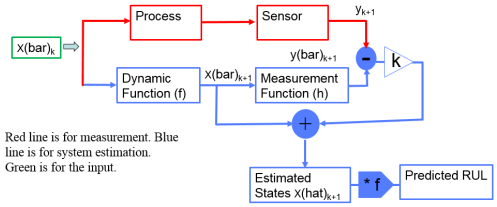

Figure 22: State Estimation Process

The advantage of the estimator over other techniques is ~~the~~ that there is no need for the specified dominant model from the undying physics. By observing the measurement data, the undying model can be picked. It is generally accepted that the luminous flux output of LED package changes in the exponential pattern with aging time as the model used in TM21 method. The following equation shows the transfer function based on the exponential model.

$$\begin{bmatrix} x_1[k+1] \\ x_2[k+1] \\ x3[k+1] \end{bmatrix} = \begin{bmatrix} 1+b*\Delta t & \Delta t & x_1[k]*\Delta t \\ b^2*\Delta t & 1+b*\Delta t & 2*b*x_1[k]*\Delta t \\ 0 & 0 & 1 \end{bmatrix} * \begin{bmatrix} x_1[k] \\ x_2[k] \\ x3[k] \end{bmatrix} \quad (4)$$

Where the x1 is the measured luminous flux; x2 is the first derivative of luminous flux and x3 is the decay constant b. The fitting method is very sensitive to the experimental value. However, the data driven approach relies on the analysis of the in situ monitored data obtained from the experiment which can eliminate the noise by passing the data through the filter first. Figure 23 shows the filtered data vs the experimental data.

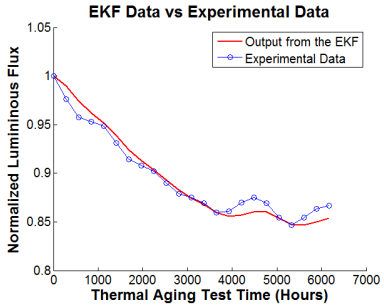

Figure 23: Comparison between the Filtered Data with the Experimental Data taken at 105°C

Luminous flux is changing exponentially with aging time. However, remaining useful life (RUL) is a linear function in terms of the thermal aging time. The following Figure 24 shows the projection of luminous flux and the calculation of RUL.

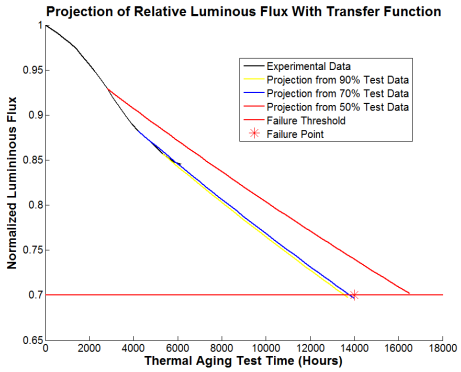

Figure 24: Projection of Relative luminous flux and the Calculation of RUL

The RUL can be calculated by projecting the state vector forward at each measurement point until it crosses the threshold [24-25]. The time between the start point of the projection and the intersection is the RUL which is shown in the previous Figure 24. ~~Plot~~ Plotting the ideal RUL in terms of thermal aging time will give a straight line with a slop of 135° (the red line in Figure 25). The following Figure 25 shows the RUL prediction with the station estimation method. The red line is the ideal RUL and the black line is the predicted RUL. The blue line is the ± 20% error boundary.

The result shows that all predicted~~ion~~ results can fall into the 20% boundary of the goal after 3000 hours. Also, the prediction aligns with the ideal data after 4000 hour's data. It can be seen that the implement of state estimator is easier than the TM21 protocol in that it requires less test time.

Commented [DL2]: Slope is defined as Δy/Δx. Since both parameters in Figure 25 are time in hours, the slope of Figure 25 has no units. I do not know where the degree units come from for the slope unless you are referring to the angle that the line makes with the x axis. This is not really the proper way to describe the slope.

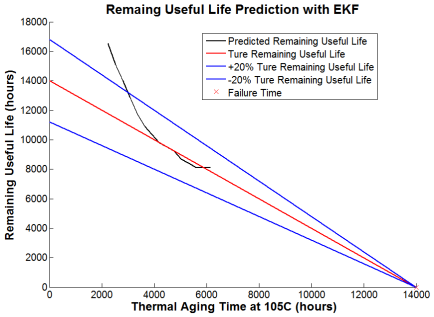

Figure 25: Predicted RUL vs the Ideal RUL

However, there are several disadvantages of state estimation. It is not be able to predict the luminous flux at the other test conditions, while, the TM21 can predict the luminous flux at any given condition with two given test conditions. The possible solution for this tradeoff is to combine the TM21standard with the state estimation. State estimation method can predict the decay constant and the projected initial constant with very less data, comparing with 6000 hours' data required by TM21. Then, the predicted decay constant can be used to calibrate the activation energy. The last part of TM21 method then can be finished with the calculated activation energy.

CONCLUSION

Pc-HB warm white LEDs used in LED based products are able to deliver high CRI, high energy efficiency and long lifetime in both daily and industry applications. While previous studies and test standards have focused on the degradation mechanisms caused by high temperature, this study includes the analysis of the relative humidity effects on the LED package. A detailed comparison of the failure mechanisms caused by the relative humidity and the thermal stress is performed in this paper. The measurements of different parameters show that different ambient environment will lead to different failure modes. Temperature and humidity have totally different effects on the warm white LED package. Test result from this study demonstrates that humidity can alter the phosphor and binder layer that sit on top of the blue photon emitter. Also, analysis in this study and the previous study show that high ambient temperature degrades the optical parts of the package and leads to the reduction of luminous flux. If the junction temperature goes across the limit, the contact resistance of the diode will go up and lead to a VI curve shift. Consequently, the package will fail catastrophically, due to the accumulated heat. Besides, a state estimation approach has been developed to predict the RUL of LED packages. During the estimation, the measured luminous flux is used to train the state estimator and predict the state in the future. Compared with TM21 standard, the proposed method is easier to implement and time saving. In conclusion, a perspective that takes into account the effects of both relative humidity and thermal stress is essential for the designers to improve the reliability of LED based products.

ACKNOWLEDGE

The work presented here in this paper has been supported by a research grant from the Department of Energy under Award Number DE-EE0005124. The authors would like to acknowledge Michael Bozack, Bart Prorok for their technical and editorial assistance.

REFERENCE

[1] Dupuis, R.D. and Krames, M.R., History, development, and applications of high-brightness visible light-emitting diodes. Journal of Lightwave Technology, 26(9), pp.1154-1171, 2008.

[2] Luo, H., et al., Analysis of high-power packages for phosphor-based white-light-emitting diodes. Applied physics letters, 86(24), p.243505, 2005.

[3] Setlur, A., Phosphors for LED-based solid-state lighting. The Electrochemical Society Interface, 16(4), p.32, 2009.

[4] Lall, P., et al., LED Lumen Degradation and Remaining Life Under Exposure to Temperature and Humidity. In ASME 2013 International Mechanical Engineering Congress and Exposition, pp. V010T11A076-V010T11A076, November 2013.

[5] Lall, P., et al., Failure mechanisms and color stability in light-emitting diodes during operation in high-temperature environments in presence of contamination. In Electronic Components and Technology Conference (ECTC), pp. 1624-1632, May 2015.

[6] Lall, P., et al., Prognostics Health Management Model for LED Package Failure Under Contaminated Environment. In ASME 2015 International Technical Conference and Exhibition on Packaging and Integration of Electronic and Photonic Microsystems collocated with the ASME 2015 13th International Conference on Nanochannels, Microchannels, and Minichannels, pp. V002T02A047-V002T02A047, July 2015.

[7] Lall, P., et al., Assessment of Lumen Degradation and Remaining Life of Light-Emitting Diodes Using Physics-Based Indicators and Particle Filter. Journal of Electronic Packaging, 137(2), p.021002, 2015.

[8] Meneghini, M, et al., High-temperature degradation of GaN LEDs related to passivation. Electron Devices, IEEE Transactions on, 53(12), pp.2981-2987, 2006.

[9] Meneghini, M., et al., Stability and performance evaluation of high-brightness light-emitting diodes under DC and pulsed bias conditions. SPIE Optics+ Photonics. International Society for Optics and Photonics, pp. 63370R-63370R, 2006.

[10] Meneghini, M., et al., Reversible degradation of ohmic contacts on p-GaN for application in high-brightness LEDs. IEEE Trans. Electron Devices, vol. 54, no. 12, pp. 3245–3251, Dec 2007.

[11] Meneghini, M., et al, A review on the reliability of GaN-based LEDs. Device and Materials Reliability. IEEE Transactions on. 8(2):323-31, Jun 2008.

[12] N. Narendran*, et al., Solid-state lighting failure analysis of white LEDs. Journal of Crystal Growth, Volume 268, Issues 3–4, Pages 449–456, August 2004.
[13] X. A. Cao, et al., Defect generation in InGaN/GaN light-emitting diodes under forward and reverse electrical stresses. Microelectron. Reliab., vol. 43, no. 12, pp. 1987–1991, Dec 2003.
[14] Egawa, T., et al., Characteristics of InGaN/AlGaN light-emitting diodes on sapphire substrates. Journal of applied physics 82, no. 11: 5816-5821, 1997.
[15] Davis, J.L., et al., System reliability for LED-based products. In Thermal, mechanical and multi-physics simulation and experiments in microelectronics and microsystems (eurosime), pp. 1-7, April 2014.
[16] Davis, J.L., et al., Insights into accelerated aging of SSL luminaires. In SPIE Optical Engineering+ Applications, pp. 88350L-88350L, September 2013.
[17] IESNA Testing Procedures Committee, Approved Method: Measuring Lumen Maintenance of LED Light Sources. IESNA LM-80-08. Illuminating Engineering Society of North America. New York, 2008.
[18] Electrical and Photometric Measurements of Solid-State Lighting Products, IES-LM-79-08, 2008.
[19] Specifications for the Chromaticity of Solid State Lighting Products: For Electric Lamps, ANSI_ANSLG C78.377-2011. National Electrical Manufacturers Association/American National Standard Lighting Group, 2011
[20] Gernot Hoffmann, Graphics for Color Science, 2004
[21] J. Schanda, Colorimetry: Understanding the CIE System. Hoboken, NJ, USA: Wiley, 2007.
[22] Illuminating Engineering Society of North America, Projecting long term lumen maintenance of LED light sources. (2011): 25. 2011.
[23] Lall, P., et al, Comparison of particle filter using SIR algorithm with self-adaptive filter using ARMA for PHM of Electronics. In Thermal and Thermomechanical Phenomena in Electronic Systems (ITherm), pp. 1292-1305. 2012.
[24] Saxena, A., et al., On Applying the Prognostics Performance Metrics. Annual Conference of the PHM Society, vol 1, 2009.
[25] Saxena, A., et al., Metrics for Evaluating Performance of Prognostic Techniques. Intl. Conf. on Prognostics and Health Management, pp. 1-17, October 2008b.